ELSEVIER

Materials Science and Engineering A290 (2000) 190–197

MATERIALS SCIENCE & ENGINEERING A

www.elsevier.com/locate/msea

Roughness and oxidation: application to NiO growth on Ni at 800°C

A.M. Huntz *, B. Lefevre, F. Cassino [1]

CNRS UMR 8647, LEMHE, University Paris Sud, 91405 Orsay, France

Received 29 September 1999; received in revised form 3 March 2000

Abstract

The changes with oxidation time of the oxide outer surface roughness, the oxide grain size and the oxidation rate constant k_c for NiO growth on Ni were studied at 800°C in 1 atm oxygen. The roughness was determined by optical interferometry establishing 2D-profiles and 3D-images. Correlations were found between the variations of the oxide outer surface roughness or the k_c values and the oxide grain size. These are attributed to the decrease of the oxide grain boundary density with time, which induces a decrease of the effective diffusion coefficient. © 2000 Elsevier Science S.A. All rights reserved.

Keywords: Nickel oxidation; NiO roughness; Oxidation constant; Oxide grain size

1. Introduction

The growth of NiO has been extensively studied [1,2] mainly because thermal oxidation of nickel gives NiO as the only oxide compound in the film. This offers the possibility of exploring, in a very wide range of temperatures, the Ni–NiO system which is of great technical importance because nickel is used as the basis or as a major component of numerous alloys for high temperature applications. So, this system is often chosen as a model system [3,4]. One remaining question concerns the relationships between the surface roughness of both the metal and the oxide and the oxidation kinetics and its mechanism. Only a few papers deal with this problem, but it can be expected from Czerwinski et al. [5–7] that relationships exist between the change of the topography of the oxide | gas interface and the mechanism of oxide growth. One other interest is that oxide growth, as a diffusion controlled phenomenon, could generate complex surfaces with fractal features [8].

In this work, our goal is to give information about the NiO surface roughness in comparison with parameters which characterise both the oxidation rate (k_p) and the microstructure of the oxide film (particularly the oxide grain size).

2. Experimental

The composition of nickel is given in Table 1. Samples of (10 × 10 × 1 mm) were prepared and heated in a high vacuum in order to stabilise the microstructure. Then, most of the samples were mechanically polished up to 3 μm diamond paste (or 3 μm diamond spray in order to compare). Some were chemically polished and etched at 85°C in a bath consisting of 30% HNO_3, 10% H_2SO_4, 50% CH_3COOH and 10% H_2O. The average grain size of Ni is about 175 μm. Thermogravimetric tests (sensitivity of 1 μg) were performed in 1 atm oxygen mainly at 800°C. The sample was heated in the oxidation chamber during 15 min and further results were corrected from the oxidation occurring during this step.

Optical interferometry was performed with a MICROXAM profilometer to obtain surface maps, line segment profiles, 2D-profiles and 3D-images, and to evaluate the roughness of the outer surface of the oxide films on the post-oxidised Ni samples. After each oxidation time at 800°C, ranging from 15 min to 24 h,

* Corresponding author. Tel.: +33-1-69-156318; fax: +33-1-69-154819.

E-mail address: am.huntz@lemhe.u-psud.fr (A.M. Huntz).

[1] Present address: Departamento de Fisica, Universidade Federal de Ouro Preto, 35.400-000, Ouro Preto, MG, Brazil.

PII: S0921-5093(00)00944-8

Table 1
Nickel composition (provided by Goodfellow)

Element	Cu	Fe	Mg	Mn	Si	Ti	C	S
Weight (ppm)	<2500	<4000	<2000	<3500	<1500	<1000	<1500	<100

surface roughness was measured over surface areas of linear size varying from 50 to 800 μm and with a lateral resolution of the order of 0.55 μm. In these conditions, values of the average roughness R_a were measured, with

$$R_a = \frac{1}{n}\sum_{i=1}^{n}|Z_i - \bar{Z}|$$

and the average surface height

$$\bar{Z} = \frac{1}{n}\sum_{i=1}^{n} Z_i$$

The outer surface of the oxide film was observed and analysed by scanning electron microscopy (SEM) equipped with EDX.

3. Results

The oxidation rate is well represented by a complete law [3,4] given by

$$t = \frac{1}{k_l}\frac{\Delta M}{S} + \frac{1}{k_p}\left(\frac{\Delta M}{S}\right)^2 \quad (1)$$

where k_l and k_p are the oxidation rate constants of the linear and parabolic processes, respectively.

The oxide thickness is calculated by:

$$x_{ox} = \left(\frac{\Delta M \cdot M_{ox}}{S M_O \rho_{ox}}\right) \quad (2)$$

with $M_{ox} = 74.7$ g mol^{-1} the molar mass of the oxide, $M_O = 16$ g mol^{-1} the molar mass of the oxygen atom, $\rho_{ox} = 6.67$ g cm^{-3} the volumic mass of the oxide. Note that Eq. (2) assumes that the oxide occupies as much space in z direction as it needs and that it would be free of stresses [4].

If working with the oxide thickness, the parabolic oxidation rate constant k_c is deduced as:

$$t = \frac{1}{k_l'}x_{ox} + \frac{1}{k_c}(x_{ox})^2 \quad (3)$$

Fig. 1 indicates small changes in the weight gain curves according to the substrate surface preparation. Particularly, the oxide thickness on samples polished with a 3 μm diamond paste is greater than that on samples polished with 3 μm diamond spray or chemically polished. The values of the parabolic oxidation constant k_c (Eq. (3)), obtained from the curves in Fig. 1 are given in Table 2. These oxidation constant values correspond to the stable values of k_c, after ≈ 1 h oxidation.

Fig. 2 corresponds to a 3D-images of Ni surface before oxidation after a 3 μm diamond paste polishing. The morphology of the surface is approximately the same whatever the polishing mode, but the fluctuation heights varies as shown in Table 2 by the roughness values. It is also observed in this table that the greater the roughness, the greater the weight gain.

Table 3 gives the results for the roughness of the outer surfaces of NiO films obtained after oxidation at 800°C of Ni samples, previously polished with 3 μm diamond paste and oxidised during different times. The roughness was measured either on surface areas containing several grains of Ni substrate, or within a Ni grain without any grain boundary. It is worth noting that, even after 24 h of oxidation, it was possible to distinguish between the regions of the oxide film formed over the Ni grains surface and the regions of the oxide formed along grain boundaries, as shown below. Moreover, in Table 3, values obtained with two different

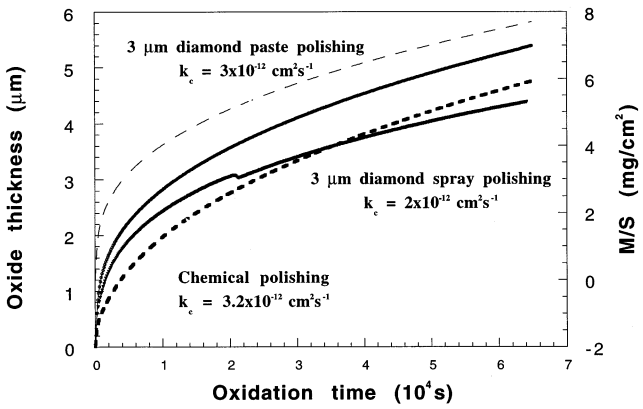

Fig. 1. Variation of the oxide thickness with the oxidation time at 800°C in 1 atm O_2. Ni substrates with various surface preparation. Oxidation in 1 atm O_2.

Table 2
Oxidation parabolic constant and R_a value for Ni oxidation at 800°C

Oxidation parabolic constant k_c (cm^2 s^{-1})	Surface preparation	R_a value (nm) before oxidation on 811.8 × 577.7 μm
3.2×10^{-12}	Chemical polishing	575.4
3.0×10^{-12}	3 μm diamond paste	30.2
2.0×10^{-12}	3 μm diamond spray	16.5

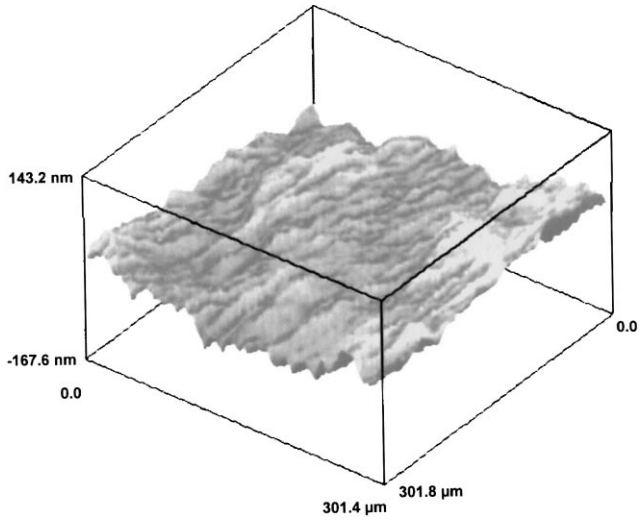

Fig. 2. 3D-images (× 10) of the non-oxidised substrate surface after 3 μm diamond paste polishing. $R_a = 17.7$ nm, area 301 × 301 μm.

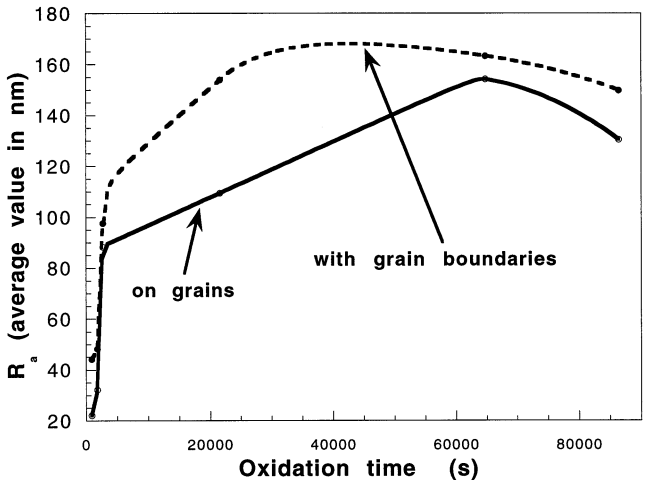

Fig. 3. Oxide surface roughness as a function of the oxidation time in 1 atm O_2. Case of nickel oxidised at 800°C after a diamond paste polishing. R_a measured on areas with and without substrate grain boundaries (× 40).

magnifications are given, i.e. with two different measuring step sizes. As it would be expected for a self-affine surface, which scales differently in vertical direction (growth direction) and horizontal directions, the roughness is slightly greater for smaller measuring step size (higher magnification). It is also observed, (Table 3 and Fig. 3), that, whatever the analysed surface portion, the oxide surface roughness increases with the oxidation time. After a given oxidation time (a few hours), the surface roughness seems to become constant. SEM observations allowed first to check that the oxide is compact and adherent and to measure the oxide grain size which evolves with the oxidation time. Fig. 4(a and b) indicate that, like the roughness, the grain size increases with increasing the oxidation time. After about 3 h oxidation, the oxide grain size does not evolve any more. Simultaneously, the oxidation rate constant determined at various oxidation times decreases at the beginning of the oxidation. The variations of these three parameters are correlated as shown in Fig. 4(c). The correlation between the roughness and the oxide grain size is due to the fact that when the oxide film grows (by predominant cationic diffusion), the oxide grain size increases and oxide crystals emergence at the outer surface increases too.

Besides, other important features of the oxide film were observed by surface analysis with optical interferometry. In particular, grain boundaries were found to be the most reactive regions of the oxidised surfaces. Fig. 5(a) clearly shows that the oxide formed over Ni grain boundaries corresponds to walls along substrate grain boundaries. To our knowledge this phenomenon was not mentioned previously. It is confirmed by the 2D-profiles in Fig. 5(b), where the distance between peaks are close to the average diameter of substrate Ni grains. It is also confirmed by SEM observations. Fig. 5(c) shows such protuberances along grain boundaries of the underlying substrate. The size of the grains formed along grain boundaries is two times smaller than the size of the grains formed on the bulk of the substrate grains. It was checked out by accurate EDX analyses that these little grains on the protuberances

Table 3
Average oxide surface roughness values for Ni samples oxidised in 1 atm oxygen at 800°C for different durations

Oxidation duration	Magnification × 10		Magnification × 40	
	R_a measured on several grains (nm)	R_a measured on one substrate grain (nm)	R_a measured on several grains (nm)	R_a measured on one substrate grain (nm)
15 min	27.0	13.8	44.1	22.2
30 min	38.2	23.9	48.2	32.2
45 min	73.9	27	97.6	88.2
6 h	75.3	35.6	153.9	109.4
18 h	106.7	74.3	163.3	154.2
24 h	135.7	99.3	149.8	130.3

developed along substrate grain boundaries are made of NiO, as the bigger grains on the bulk of the substrate grains, and not of metallic nickel. Metallic protuberances along substrate grain boundaries were suggested by works in Refs. [9,10], for instance. They were associated to internal oxidation of impurities. In our case, internal oxidation was not observed, impurities were not detected in the oxide film and the walls along grain boundaries consist in NiO. Similar phenomena can be detected on dislocation arrays of the Ni substrate, such as small angle grain boundaries and piled up dislocations. Dislocation arrays were previously detected by usual metallography of Ni samples. Fig. 6 shows enhanced oxide formation associated with a small angle grain boundary, the peak to peak distance being of the order of magnitude of the distance between dislocations observed by metallography. These phenomena justify the differences between roughness values collected in Table 3. Roughness values are greater for important surfaces containing grain boundaries or sub grain boundaries of the substrate.

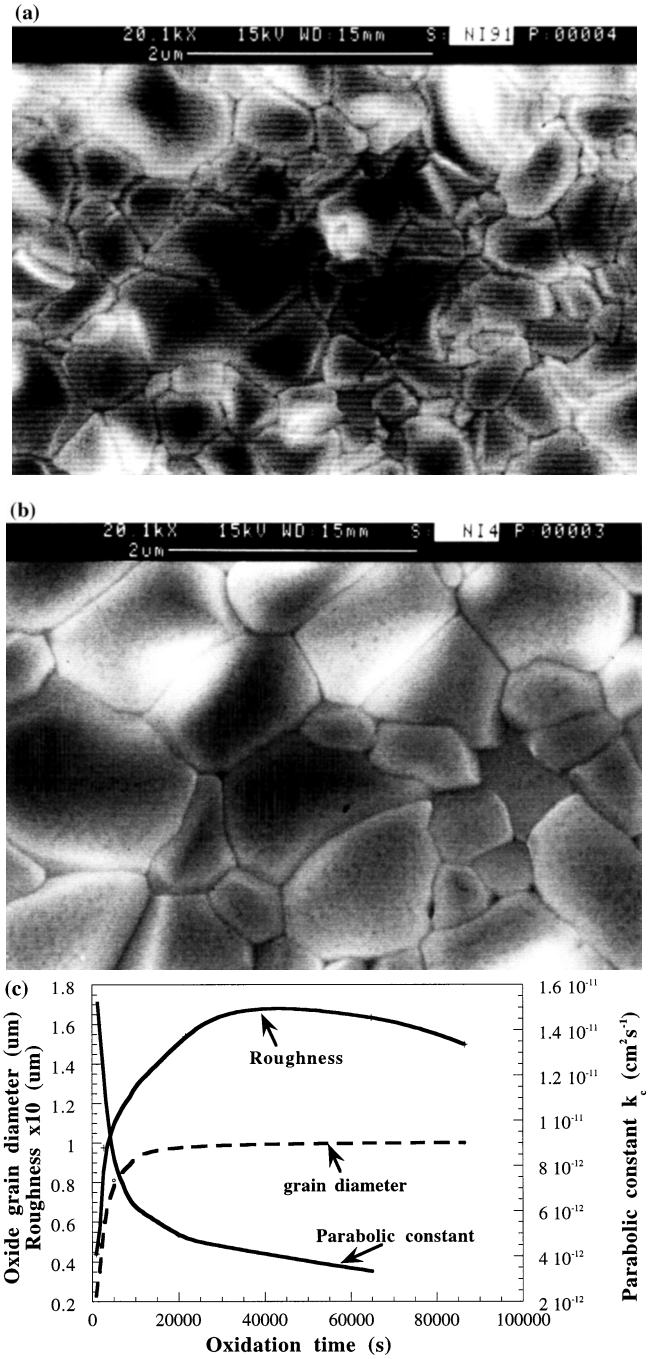

Fig. 4. (a and b) SEM images of the outer surface of the NiO oxide formed at 800°C by 45 min and 24 h oxidation, respectively. (c) Changes of the roughness, grain size and oxidation constant as a function of the oxidation time at 800°C, 1 atm O_2.

4. Discussion

Since differences between values for k_c, in Table 2, are in the range of experimental uncertainties, the long time oxidation kinetics (after 1 h) seems to be almost independent from the previous surface preparation of Ni samples. Indeed, due to the small values of R_a (expressed in nm) the substrate surface is not affected by the substrate roughness variations. It could also be thought that Eq. (1) should be continuously corrected due to the change of the oxide surface related to the oxide outer surface roughness. As suggested by [11], the outer surface A_r of a rough oxide film can be estimated by

$$A_r = \pi\phi^2/(4 + \pi\phi R_a) \quad (4)$$

ϕ being the oxide grain diameter. Thus, results in Fig. 4 allow to continuously correct the $\Delta M/S$ values assuming that S corresponds to the estimated A_r values. Once done, it leads to anomalous kinetics curves presenting a first step with weight gains and a second one with weight losses. Moreover, the experimental oxide thickness values in Fig. 1 are in good agreement with SEM observations which show oxide film thickness of the same order of magnitude than those deduced from thermogravimetric tests without any corrections of $\Delta M/S$.

In Fig. 1, it appears that after about 1 h of oxidation, the kinetic curves are almost entirely parallel. The main difference between these curves consists in different initial weight gains. This implies, as expected, that the initial surface roughness of the substrate mainly acts in the first steps of the oxidation process, enhancing the initial weight gain for initially rougher surfaces (see Table 2): the greater the Ni surface roughness, the more important the nickel amount injected in the oxide film. This is due to the fact that NiO growth is mainly ensured by cationic diffusion [2]. New oxide is formed at the oxide outer interface, but the amount of new oxide formed is related to the amount of Ni ions injected at the substrate | oxide interface.

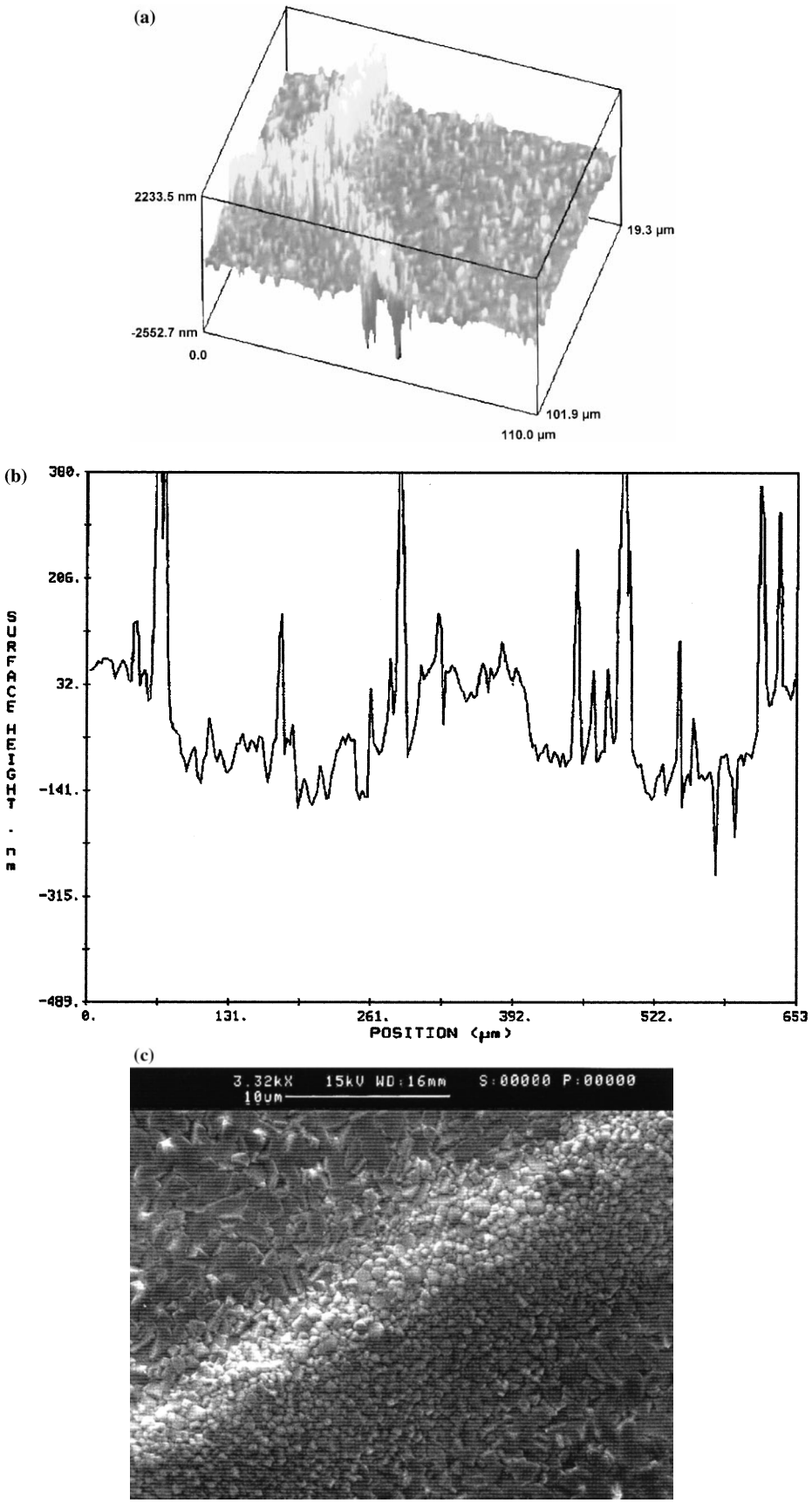

Fig. 5. (a) 3D-images (× 40) of the oxide outer surface after oxidation at 800°C for 72 h $R_a = 190$ nm, area 203×144.4 µm. (b) 2D-profile on 18 h oxidised sample (× 10), $R_a = 114$ nm, area 811.8×577.7 µm. The distance between peaks is of the same order of magnitude than the substrate grain size. (c) SEM image showing the protuberance along substrate grain boundaries and the difference in the oxide grain size according to its localisation. Ni oxidised 72 h at 800°C.

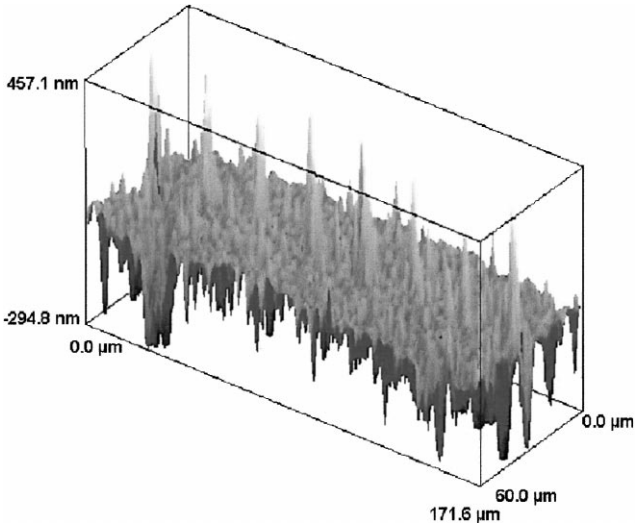

Fig. 6. 3D-image (× 40) of Ni oxidised for 15 min at 800°C after 3 μm diamond polishing suggesting an enhanced oxide growth along a dislocation wall of the underlying substrate. $R_a = 46$ nm, area 201.8 × 143.8 μm.

The k_c decrease during the first hour of oxidation, followed by the stabilisation of the oxidation rate constant (Fig. 4) indicates that grain boundary diffusion in the oxide is the predominant oxidation mechanism, as suggested in the literature [2,6,12]. Consequently, grain boundary diffusion is the predominant term in the equation giving the parabolic oxidation rate constant. Indeed, as the oxide grain size ϕ increases (Fig. 4), f, the fraction of atoms diffusing along oxide grain boundaries, commonly given by $f = 3\delta/\phi$, δ being the grain boundary width, decreases. Finally, in the expression giving the effective diffusion coefficient responsible for the oxide film growth, $D_{eff} = (1-f)D_b + fD_{gb}$ [13] (with $D_b < D_{gb}$), the second term decreases, thus k_c which is related to D_{eff} decreases also and stabilises when ϕ becomes constant. Strictly speaking, the roughness of the outer surface of the oxide film must be taken into account in the estimation of f. In the case of rough surfaces, $f = f_r$ was estimated from Ref. [11] as

$$f_r = \frac{3\delta}{\phi + 2R_a} \quad (5)$$

(Thus:

$$\frac{k_c(t_1)}{k_c(t_2)} = \frac{\phi(t_2) + 2R_a(t_2)}{\phi(t_1) + 2R_a(t_1)} \quad (6)$$

The comparison between values obtained after 15 min and 24 h of oxidation gives

$$\frac{k_c(24\text{ h})}{k_c(15')} \approx 0.17 \quad \text{when the ratio}$$

$$\frac{\phi(15') + 2R_a(15')}{\phi(24\text{ h}) + 2R_a(24\text{ h})} = 0.22$$

These two values are rather similar which confirms the influence of the oxide grain size evolution on k_c values during short oxidation times.

However, it is important to note that the contribution of the initial mass gain to the final average thickness of the oxide film does not seem negligible. For the samples mechanically polished, it amounts to $\approx 15\%$ (Fig. 1). These differences in thickness may play some role in the mechanical behaviour of the oxide films, under thermo-mechanical loading. This is a very important point in high-temperature alloy protection.

Comparing our results with those obtained in Refs. [5–7], it appears that for undoped nickel a change of the oxide surface roughness R_a is similarly observed. But, in our work, a stabilisation of the roughness occurs associated with the oxide grain growth and, consequently, with the oxidation constant. Moreover, a linear variation of R_a/x_{ox} versus x_{ox} was not observed in our case.

Another important point is that enhanced oxidation is observed, by optical profilometry and by SEM, along grain boundaries and dislocation walls of the substrate. Thus, contrarily to [6], it can be said that linear and planar defects of the substrate have an effect.

It is now interesting to analyse these results in the light of the fractal theory which can allow to predict the surface change by a scale transformation. The oxide film is characterised by a preferential growth direction, so the growth behaviour should be different along the direction perpendicular to the film, compared to the direction in the plane of the film during an isotropic scale transformation. Basically, the idea of fractal properties of roughness relies on the fact that the estimated value of roughness depends on the size of the measuring element, which is the case here (Fig. 7). Indeed, the roughness dependence on the linear size L of the observed oxide surface was analysed in the range $50 < L < 800$ μm. The chosen range for L has some interest because it contains the average grain size of Ni substrate (≈ 175 μm). The results in Fig. 7 suggest that

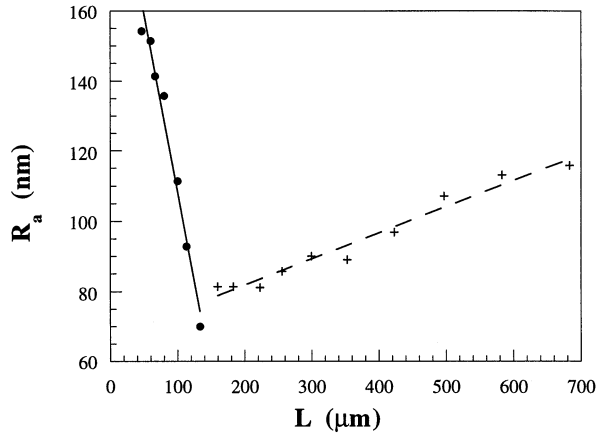

Fig. 7. Oxide surface roughness as a function of the linear length. Oxidation at 800°C for 45 min, magnification × 10, area 811.8 × 577.7 μm.

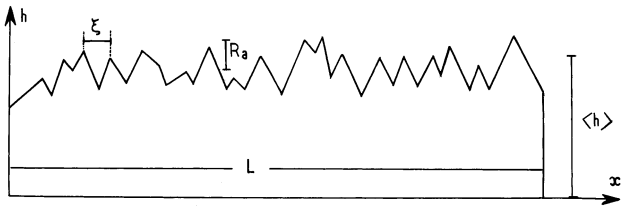

Fig. 8. Parameters describing a fractal surface [16].

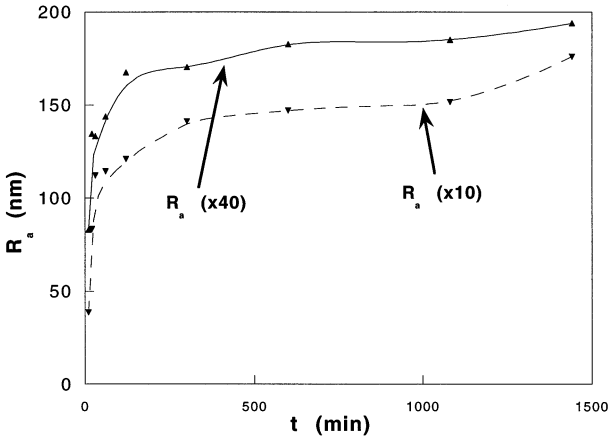

Fig. 9. R_a of the NiO outer surface for different observation sizes versus the oxidation time of Ni at 800°C.

Table 4
Values of the β exponent ($R_a \propto t^{\beta}$), of $R_{a(sat)}$ and t_{sat} (deduced from Fig. 9).

	Magnification × 10	Magnification × 40
β	0.21	0.13
$R_{a(sat)}$ (nm)	146	166
t_{sat} (min)	293	134

two roughness behaviours occur for two different scale domains, with a crossover close to the average grain size of the substrate.

In order to characterise a fractal surface, several parameters must be considered [14] (Fig. 8): the fractal local dimension which characterises the variation of a measurement during a scale transformation, the linear length L, the roughness R_a and the correlation length ξ which corresponds to the average distance between two peaks. The theory of fractal surface growth indicates that the two last parameters vary with the growth time according to a power law [15,16]: $R_a \propto t^{\beta}$ for $t < t_{sat}$, t_{sat} being the time at which R_a takes a constant value $R_a(s_{at})$, and $R_a = R_a(s_{at})$ for $t \geq t_{sat}$.

Moreover, the roughness and the saturation time depend on the measuring step size L, i.e. on the size of the linear length of the observed surface: $R_a(s_{at}) \propto L^{\alpha}$ and $t_{sat} \propto L^{z}$ with $z = \alpha/\beta$.

The exponents α, β and z characterise the surface and are called scale exponents.

The variations of the oxide surface roughness with the oxidation time for various measuring steps are collected in Fig. 9. The fittings of $R_a = f(t)$ with a power law are not very satisfying, but values of the exponent β are given in Table 4. β is positive as the roughness increases with the oxidation time. Such curves allow to determine with a relative uncertainty $R_a(s_{at})$ and t_{sat} whose values are given in Table 4. If t_{sat} increases with L, the linear length of the observed surface, R_{sat} decreases with L. This would mean that the exponent z is positive while the exponent α is negative which is not coherent with the positive value of the exponent β.

Thus, on the basis of the obtained results, it is not possible to conclude on the fractal character of NiO growth, probably because the surface behaves differently according to the value of L for the measurements (see Fig. 7).

5. Conclusions

The study of the parabolic oxidation rate constant k_c for the NiO growth on Ni at 800°C, of the oxide grain size and of the outer surface roughness with oxidation time led to the following remarks.

During the first hour of oxidation, these parameters change and then stabilise: k_c decreases while the oxide grain diameter ϕ and the oxide outer surface roughness increase. The k_c decrease is correlated to the f increase, i.e. to the decrease of the oxide grain boundary density which induces a decrease of the effective diffusion coefficient in the oxide film.

At the beginning of the oxidation, there is a difference in the oxidation rate according to the substrate polishing conditions. The greater the substrate surface roughness, the greater the oxidation rate, due to the enhancement of the amount of Ni injection in the oxide films.

The oxidation rate does not depend on the roughness of the oxide outer surface.

Enhanced oxidation is observed along grain boundaries and dislocation walls of the substrate.

The oxide surface roughness changes with the oxidation time until it reaches a saturation value. It also evolves with the linear length of the observed surface and two domains are observed for this variation.

Acknowledgements

Thanks are due to F. Kherbouche and B. Poumellec who gave us advice on the use of the interferometric profilometer in 'Chimie des Solides' Laboratory, Orsay, and to D. Deydier who performed some of the experiments

References

[1] P. Kofstad, High Temperature Corrosion, Elsevier Applied Science, New York, 1988.
[2] A. Atkinson, Rev. Mod. Phys. 57 (1985) 437.
[3] D. Monceau, B. Pieraggi, Oxid. Met. 50 (1998) 477.
[4] A.M. Huntz, J. Mater. Sci. Lett. 18–24 (1999) 1981.
[5] F. Czerwinski, W.W. Smeltzer, J. Electrochem. Soc. 140 (1993) 2606.
[6] F. Czerwinski, J.A. Szpunar, R.G. Macaulay-Newcombe, W.W. Smeltzer, Oxid. Met. 43 (1995) 25.
[7] F. Czerwinski, J.A. Szpunar, Corr. Sci. 39 (1997) 147.
[8] J.F. Gouyet, M. Rosso, B. Sapoval, in: A. Bunde, S. Havlin (Eds.), Fractal Surfaces and Interfaces, in Fractals and Disordered Systems, second ed., Springer-Verlag, Berlin, 1996.
[9] H.C. Yi, S.W. Guan, W.W. Smeltzer, A. Petric, Acta Metal. Mater. 42 (1994) 981.
[10] Y. Shida, F.H. Stott, B.D. Bastow, D.P. Whittle, G.C. Wood, Oxid. Met. 18 (1982) 93–127.
[11] S.C. Tsaï, A.M. Huntz, Oxid. Met. 43 (1995) 581.
[12] W.W. Smeltzer, D.J. Young, Prog. Solid State Chem. 10 (1975) 17.
[13] E.W. Hart, Acta Metal. 5 (1957) 597.
[14] A. Bunde, S. Havlin (Eds.), Fractals in Science, Springer-Verlag, Berlin, 1994.
[15] X.Y. Lei, P. Wan, C.H. Zhou, N.B. Ming, Phys. Rev. E 54 (1996) 5298.
[16] A.L. Barabasi, H.E. Stanley, Fractal Concepts in Surface Growth, Cambridge University, Cambridge, 1995.